On the role of vortex stretching in energy optimal growth of three-dimensional perturbations on plane parallel shear flows

H. Vitoshkin[1]†**, E. Heifetz**[2]**, A. Yu. Gelfgat**[1] **and N. Harnik**[2]

[1] School of Mechanical Engineering, Faculty of Engineering, Tel Aviv University, Tel Aviv 69978, Israel

[2] Department of Geophysics, Atmospheric and Planetary Sciences, Tel Aviv University, Tel Aviv 69978, Israel

The three-dimensional linearized optimal energy growth mechanism, in plane parallel shear flows, is re-examined in terms of the role of vortex stretching and the interplay between the spanwise vorticity and the planar divergent components. For high Reynolds numbers the structure of the optimal perturbations in Couette, Poiseuille and mixing-layer shear profiles is robust and resembles localized plane waves in regions where the background shear is large. The waves are tilted with the shear when the spanwise vorticity and the planar divergence fields are in (out of) phase when the background shear is positive (negative). A minimal model is derived to explain how this configuration enables simultaneous growth of the two fields, and how this mutual amplification affects the optimal energy growth. This perspective provides an understanding of the three-dimensional growth solely from the two-dimensional dynamics on the shear plane.

Key words: shear waves, vortex instability, low-dimensional model

1. Introduction

It is well-known that three-dimensional (3D) perturbations at incompressible, high Reynolds number, on plane parallel shear flows, attain non-modal growth which may be much larger than the growth attained by two-dimensional (2D) perturbations that are confined to the shear plane, e.g. Butler & Farrell (1992) and Reddy & Henningson (1993) for Couette and Poiseuille shear flows. The 3D growth appears at later stages when the perturbations are tilted with the background shear. This stands in contrast to the 2D optimal growth which is obtained when the perturbations are tilted against the shear. In 2D, the perturbation in the energy norm grows via the Orr mechanism, Orr (1907), and in the presence of an inflection point, by the action at a distance between counter-propagating Rossby waves, Heifetz & Methven (2005). The 3D growth mechanism is commonly rationalized by the lift-up mechanism, Ellingsen & Palm (1975), Landahl (1980), Schmid & Henningson (2001), which can also be viewed as a tilt-up of the spanwise background vorticity by the cross-stream perturbation velocity, Farrell & Ioannou (1993). This explanation follows the mathematical procedure by

which the dynamics is usually resolved: a homogeneous equation for the cross-stream velocity is derived, and the spanwise variation of this velocity serves as a source for the tilt-up of the background vorticity. However, since in planar 2D dynamics there is no spanwise variation and the cross-stream vorticity is zero by definition, it is difficult to compare the 2D and the 3D optimal dynamics from the lift-up perspective.

Nonetheless, the third dimension adds a fundamental mechanism which is absent from strictly 2D flow: the background shear vorticity (pointing by definition in the spanwise direction) may be stretched due to contraction of areas in the shear plane by the planar divergence of the shear plane projection of the perturbation field (d). This implies generation of the spanwise component of the vorticity perturbation (q). Thus, the perturbation divergence and vorticity scalar fields evolve together, and we expect optimal growth to occur when the interplay between d and q results in a simultaneous growth of the two fields. Since the circulation associated with q is on the shear plane, the interplay between d and q is expected to provide an understanding of the 3D optimal growth solely in terms of the 2D planar perturbation dynamics.

In §2 we show that it is a robust feature that the largest 3D growth is obtained when d and q are in (anti) phase in regions of positive (negative) mean shear. Furthermore, the fastest growing perturbations resemble localized plane waves that are tilted with the local maximal shear and this behaviour is insensitive to the shear curvature. In §3 we therefore derive a plane-wave minimal model for the interplay between d and q in the presence of a constant background shear. In §4 the optimal growth in the energy norm is analysed from this d–q perspective, and in §5 we conclude and discuss our results.

2. Numerical comparison between 2D and 3D growth

We define the Cartesian coordinates $r = (x i, y j, z k)$ as the (streamwise, cross-stream, spanwise) directions so that the background shear velocity is $\overline{U} = \overline{U}(y) i$, the perturbation velocity vector is $u = (u, v, w)$, the perturbation spanwise vorticity is $q = (\partial v/\partial x) - (\partial u/\partial y)$, and the 2D divergence field on the shear plane is $d = (\partial u/\partial x) + (\partial v/\partial y)$.

In figure 1 we present the optimal evolutions of 2D and 3D perturbations in plane parallel bounded Couette and Poiseuille shear flows, as well as in an open mixing-layer profile for relatively high Reynolds numbers ($Re = 5000, 1000, 5000$, respectively), but below the critical values enabling modal instability. The first two examples are in excellent agreement with the results of Reddy & Henningson (1993), whereas the calculations of the last are new (to the best of our knowledge). The optimal vectors of the perturbations are represented as Fourier modes in the streamwise and spanwise directions ($\propto e^{i(kx+mz)}$). In the cross-stream direction the perturbations are discretized and resolved by central finite-difference schemes in the same way as in Gelfgat & Kit (2006). For the three profiles the 3D maximal growths are indeed larger by an order of magnitude than the corresponding 2D ones, and are attained at later stages. The q contours indicate that in all cases the eddies are initially tilted against the shear, and then they evolve to become more aligned.

The major difference between the growth evolution of 2D and 3D flows is that in the former, the maximum energy value is obtained when the eddies are aligned perpendicular to the shear, whereas in the latter it is obtained when the eddies are tilted with the shear. For the 3D perturbations, the contours of d are superimposed (for 2D perturbations d is zero since incompressibility is assumed). It is evident for
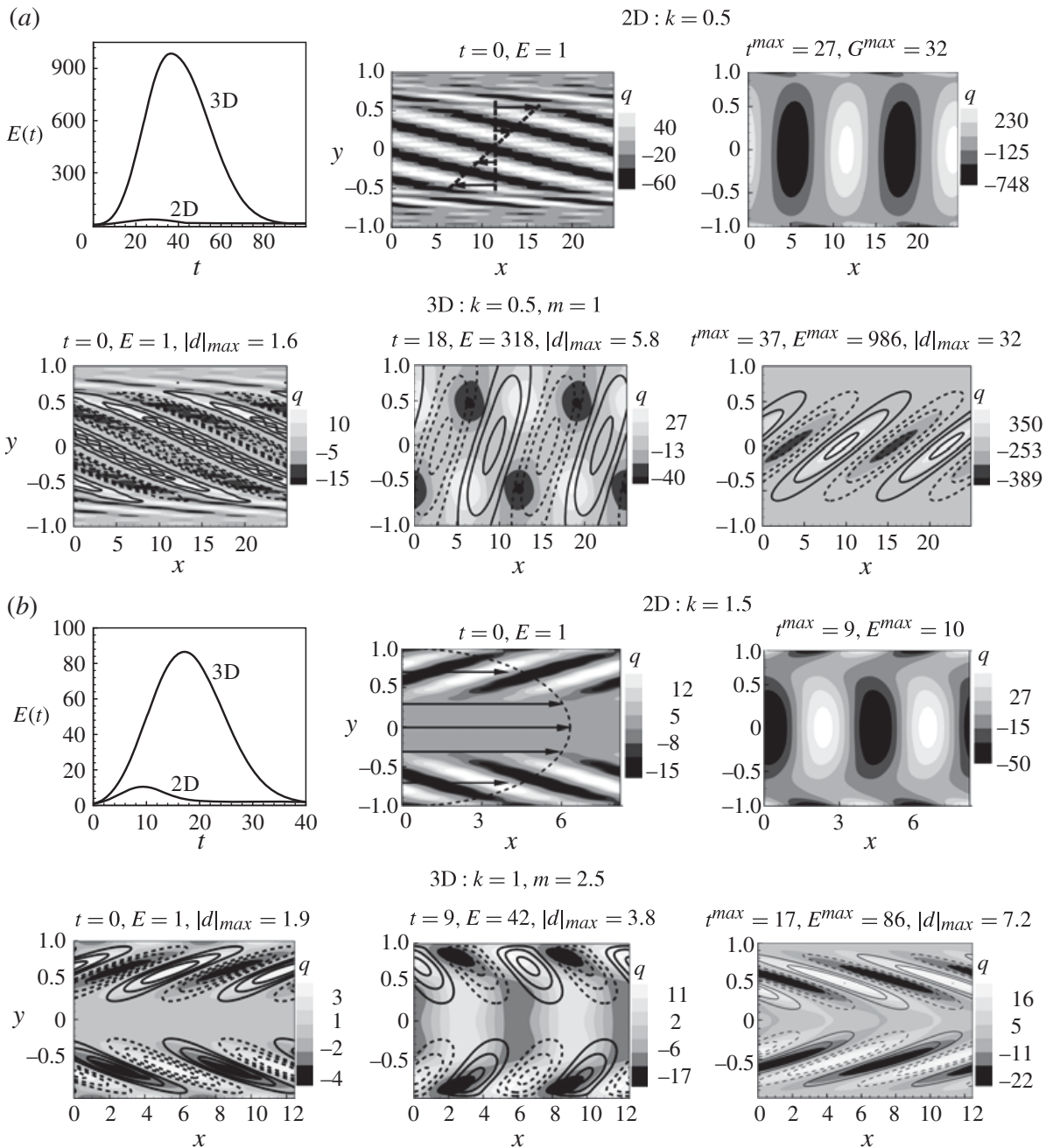
FIGURE 1. For caption see next page.

the three profiles that when the eddies experience their largest 3D growth, d and q are in (anti) phase when the mean shear is positive (negative), and the perturbation structures resemble localized plane waves that are tilted with the local maximal shear. These structures are robust and were found in many different Fourier modes of the three canonical profiles. Therefore, it seems that at the stage of optimal growth the exact curvature of the shear profile is not very important. Furthermore, the effect of rigid boundaries is not essential as the plane-wave-like structures are located well within the domain. Since the Reynolds numbers are relatively high, dissipation also has a relatively small effect during the growth stage. Thus, in the following section the essence of the d–q interaction is examined in a minimal model of an inviscid plane wave in the presence of a constant unbounded background shear.
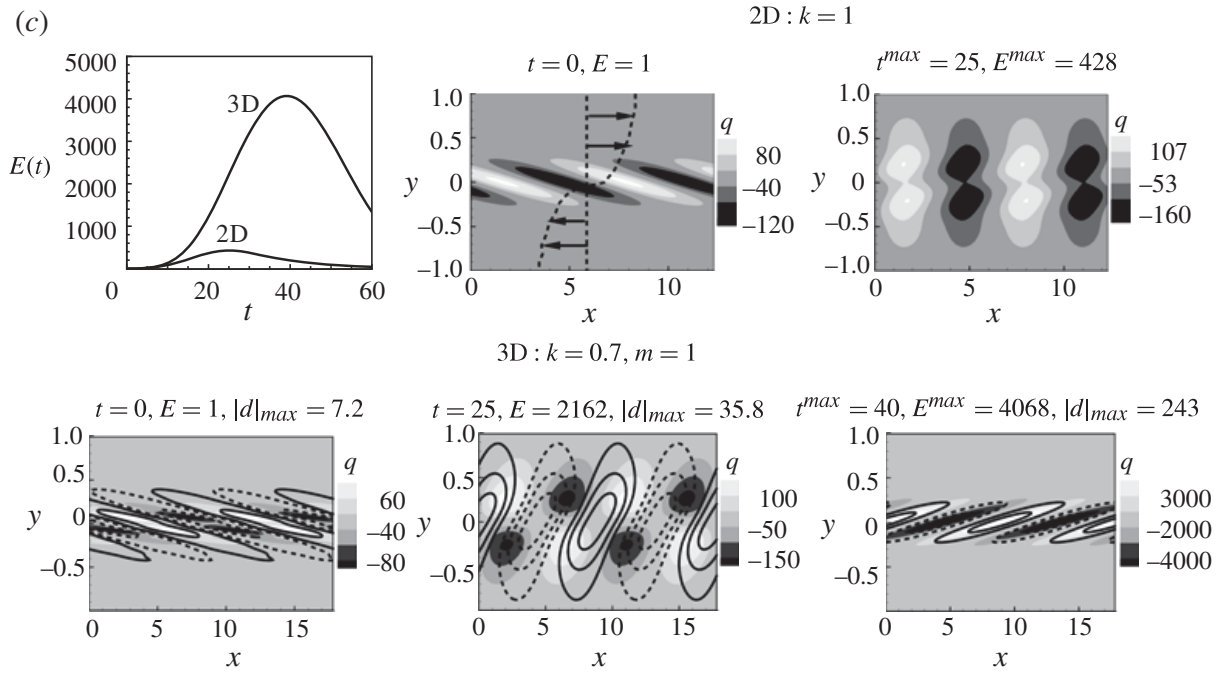
(c)

2D : $k = 1$

3D : $k = 0.7$, $m = 1$

FIGURE 1. (cntd). Optimal energy growth for 2D and 3D perturbations on Couette *(a)* Poiseuille *(b)* and mixing layer *(c)* plane parallel shear flows for relatively high Reynolds numbers ($Re = 5000, 1000, 5000$, respectively). The different streamwise and spanwise wavenumbers (k, m) are selected to generate maximal non-modal growth. Solid curves indicate the energy growth evolution, $E(t)$, from the initial optimal perturbations. Note that $E_{3Dmax} \gg E_{2Dmax}$ and $t_{3Dmax} > t_{2Dmax}$, where t_{max} is the time of maximal amplification over all times. The structure of the optimal perturbations at selected times is indicated by the contours of the spanwise vorticity q. For the 3D perturbations the planar divergent field d is superimposed and indicated by the solid (positive) and dashed (negative) contours. Note that in 2D, E_{max} is obtained when the eddies are aligned perpendicular to the shear, whereas in 3D it occurs when the eddies are tilted with the shear, and d and q are in (anti) phase when the mean shear is positive (negative). Furthermore, the structures resemble localized plane waves that are tilted with the local maximal shear.

3. An analytical model of 3D plane-wave growth in constant shear

We consider an unbounded Eulerian flow with a constant background shear $\overline{U}(y) = \Lambda y$, where $\Lambda = (\partial \overline{U}/\partial y) = -\overline{q}$, and $\overline{q}$ is the background vorticity, pointing in the spanwise direction. Since in most regions of the three canonical examples the background shear is positive, Λ is taken to be a positive constant and therefore the background spanwise vorticity $\overline{q}$ is negative. The linearized eddy momentum equation can then be written as:

$$\frac{\mathrm{D}\boldsymbol{u}}{\mathrm{D}t} = -\boldsymbol{\nabla}p - \Lambda v\boldsymbol{i} \tag{3.1}$$

where p is the perturbation pressure divided by the constant density of the flow, and $\mathrm{D}/\mathrm{D}t = (\partial/\partial t) + \Lambda y((\partial/\partial x))$ is the linearized Lagrangian derivative.

In the absence of dissipation, conservation of circulation implies that when d is positive the absolute value of the spanwise vorticity decreases. Since $\overline{q}$ is negative, a positive anomaly of q should be generated when d is positive (figure 2*a*):

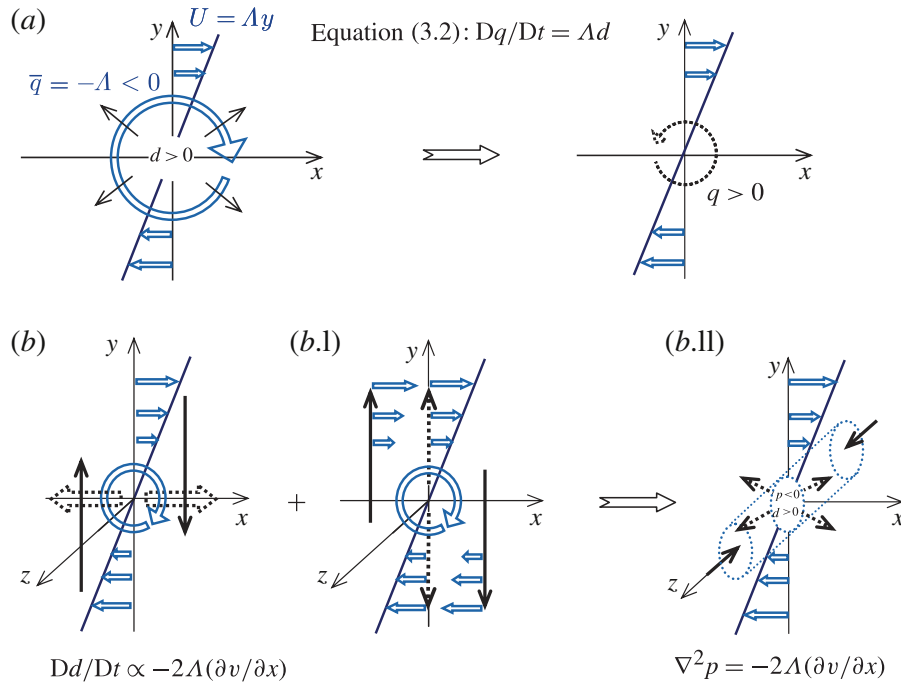$$\frac{\mathrm{D}q}{\mathrm{D}t} = \Lambda d. \tag{3.2}$$

FIGURE 2. (Colour online) Graphical interpretation of the dynamical processes described in (3.2)–(3.4). Doubled and bold single arrows represent the background and the perturbation flows, respectively. Dashed arrows represent the result of the process. (*a*) Equation (3.2): conservation of circulation implies that an area expansion in the shear plane by the planar divergent field perturbation *d* decreases the spanwise vorticity. Since the background vorticity $\bar{q}$ is negative, expansion generates a positive spanwise vorticity perturbation *q*. (*b*) The second term on the right-hand side of (3.3) for $(\partial v/\partial x) < 0$: generation of *d* by differential advection of the mean flow by the cross-stream perturbation velocity (*b*.I), together with differential advection of the cross-stream perturbation velocity by the mean flow (*b*.II). Equation (3.4) and incompressibility imply that expansion in the shear plane results in a shrinking in the spanwise direction, due to a negative pressure perturbation. Therefore, for a positive background shear sign(*p*) = sign($(\partial v/\partial x)$) and the two terms on the right-hand side of (3.3) are of opposite sign, with the latter dominating.

Thus, in order to obtain growth in *q*, *q* and *d* should be positively correlated. On the other hand, the divergence tendency equation, obtained from (3.1), is:

$$\frac{\mathrm{D}d}{\mathrm{D}t} = -\nabla_2^2 p - 2\Lambda\frac{\partial v}{\partial x} \qquad (3.3)$$

where $\nabla_2^2 = (\partial/\partial x^2) + (\partial/\partial y^2)$ is the 2D Laplacian on the shear plane. The first term on the right-hand side indicates that *d* will grow when the planar Laplacian of the pressure anomaly is positive. The second term shows the contribution of differential advection to *d*. The factor of 2 stems from the separate contributions of the differential advection of the mean flow by the cross-stream perturbation velocity, and the differential advection of the cross-stream perturbation velocity by the mean flow (figure 2*b*). Incompressibility ($\nabla \cdot \boldsymbol{u} = 0$) determines, however, that when *d* increases

the pressure anomaly is negative since:

$$\frac{\mathrm{D}d}{\mathrm{D}t} = -\frac{\mathrm{D}}{\mathrm{D}t}\frac{\partial w}{\partial z} = \frac{\partial^2 p}{\partial z^2}. \tag{3.4}$$

This somewhat counter-intuitive behaviour is simply because a divergent motion in the shear plane must be accompanied by a shrinking in the spanwise direction. The latter can only result from a negative pressure anomaly. This implies that the two terms on the right-hand side of (3.3) must be of opposite sign, with the latter dominating.

The 2D shear-deformed plane-wave solution, presented originally by Orr (1907), can be generalized straightforwardly to 3D: $\chi(\boldsymbol{r}, t) = \hat{\chi}(t)e^{i\boldsymbol{K}\cdot\boldsymbol{r}}$, where the 3D wavenumber vector $\boldsymbol{K} = (k, l = l_0 - k\Lambda t, m)$, and $\mathrm{D}\chi/\mathrm{D}t = (\mathrm{d}\hat{\chi}/\mathrm{d}t)e^{i\boldsymbol{K}\cdot\boldsymbol{r}}$. Then the right-hand side of (3.3) can be expressed in terms of q and d. Since (3.3) and (3.4) yield the diagnostic relation, $\nabla^2 p = -2\Lambda(\partial v/\partial x)$, we can write:

$$\frac{\mathrm{D}d}{\mathrm{D}t} = -2\Lambda\left(\frac{m}{|\boldsymbol{K}|}\right)^2\frac{\partial v}{\partial x}. \tag{3.5}$$

It is now left to express v in terms of q and d by applying the 2D Helmholtz decomposition:

$$u = u_d + u_q = \frac{\partial\phi}{\partial x} - \frac{\partial\psi}{\partial y}, \quad v = v_d + v_q = \frac{\partial\phi}{\partial y} + \frac{\partial\psi}{\partial x} \tag{3.6a,b}$$

so that

$$d = \nabla_2^2\phi, \quad q = \nabla_2^2\psi. \tag{3.7a,b}$$

Equations (3.2) and (3.5) now determine the plane-wave d–q dynamics:

$$\frac{\mathrm{d}\hat{q}}{\mathrm{d}t} = \Lambda\hat{d}, \quad \frac{\mathrm{d}\hat{d}}{\mathrm{d}t} = -2\Lambda\left(\frac{m}{|\boldsymbol{K}|}\right)^2\frac{k}{(k^2+l^2)}(l\hat{d}+k\hat{q}) \tag{3.8a,b}$$

where the general solution of (3.8) is given, for completeness, in the Appendix.

We look for configurations allowing simultaneous growth in both q and d. As pointed out, (3.8a) implies that q and d must be positively correlated. For positive streamwise wavenumber k (by construction), (3.8b) indicates that $-(\partial v_q/\partial x)$ is always negative for positive q, hence while d acts to increase q, q acts to decrease d. Therefore, only the cross-stream velocity v_d, induced by the divergent field itself, can contribute to the divergent growth. Equation (3.8b) and figure 3 indicate that this may happen only when l is negative, that is when the plane wave is tilted with the shear, i.e. later than $t = l_0/(k\Lambda)$.

The d–q dynamics are reflected in the energy growth mechanism via the Reynolds stress term. The spatially averaged perturbation energy growth, obtained from the momentum equation (3.1), is:

$$\frac{\partial}{\partial t}\langle E \rangle = -\Lambda\langle uv \rangle, \quad E = \frac{|\boldsymbol{u}|^2}{2} \tag{3.9a,b}$$

where $\langle\ \rangle$ represents spatial averaging, and

$$-\langle uv \rangle = -\langle(u_q+u_d)(v_q+v_d)\rangle = -\langle(u_qv_q+u_dv_d+u_qv_d+u_dv_q)\rangle$$

$$= \frac{1}{2(k^2+l^2)^2}[kl\,|\hat{q}|^2 - kl\,|\hat{d}|^2 + l^2\mathrm{Re}(\hat{q}\hat{d}^*) - k^2\mathrm{Re}(\hat{d}\hat{q}^*)] \tag{3.10}$$

$$\langle \dot{E} \rangle = -\Lambda \langle uv \rangle = -\Lambda \langle \underbrace{u_q v_q}_{-} + \underbrace{u_d v_d}_{+} + \underbrace{u_q v_d}_{-} + \underbrace{u_d v_q}_{+} \rangle \qquad\qquad \langle \dot{E} \rangle = -\Lambda \langle \underbrace{u_q v_q}_{+} + \underbrace{u_d v_d}_{-} + \underbrace{u_q v_d}_{-} + \underbrace{u_d v_q}_{+} \rangle$$
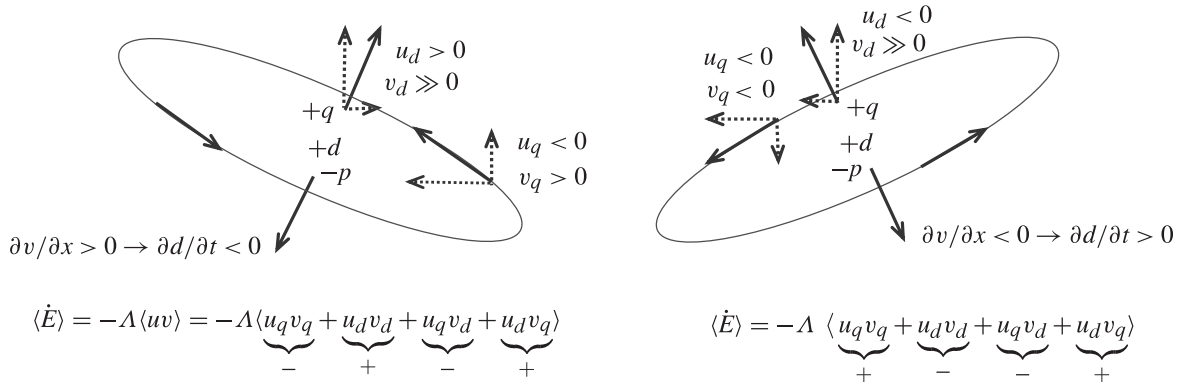
FIGURE 3. Planar divergent and rotational contributions to the 3D energy growth via the Reynolds stress mechanism, for eddies with positive spanwise vorticity, positive planar divergence and negative pressure perturbations. The contributions are illustrated for both where the eddies are tilted against and with the shear. The rotational Orr term, $-\langle u_q v_q \rangle$, is positive (negative) for negative (positive) tilt, and the divergent term, $-\langle u_d v_d \rangle$, is positive (negative) for positive (negative) tilt. The sign of the first mixed q–d term, $-\langle u_q v_d \rangle$, is always positive, whereas the second mixed d–q term, $-\langle u_d v_q \rangle$, is always negative. When the eddies are strongly tilted with the shear the latter term dominates and generates large growth that overwhelms the strong decay by the Orr mechanism. Furthermore, when the eddies are strongly tilted, $(\partial v/\partial x) < 0$, and simultaneous growth for both d and q is obtained.

where * and Re denote the complex-conjugate and the real part, respectively. The first term represents the 2D Orr mechanism which is positive (negative) when l is positive (negative), whereas the second term represents the ability of the divergent field to amplify (decay) itself for negative (positive) l. If q and d are in phase, $[\mathrm{Re}(\hat{q}\hat{d}^*) = \mathrm{Re}(\hat{d}\hat{q}^*) = |\hat{q}||\hat{d}|]$, the third mixed term is always positive but the fourth one is always negative. The signs of the different terms are evident as well from figure 3.

4. Optimal d–q dynamics in the canonical profiles

The analysis in the previous section suggests that the structure of the optimal evolution in the early and intermediate stages should not take the form of a plane wave since when $l > 0$, the increasing of q by d is accompanied by a decreasing of d by both q and d. Indeed, as indicated from figure 1, during these stages d and q depart from each other and do not resemble a plane-wave structure. This uneven interaction is expected to generate a much larger growth in q than in d, as presented in figure 4(*a*). In figure 4(*b*) the evolution of the cosine of phase shift between d and q is shown at levels where the shear is strong. Initially d and q are in phase; however while d amplifies q, both q and d act to decay d so that at some stage d changes sign and q and d become anti-phased, and then d acts to decay q. Nonetheless, at the later stage of maximum growth, q and d return to being in phase and a mutual growth is obtained when the plane-wave-like structures are tilted with the shear. Note that for a non-constant shear, (3.2) should be modified to $\mathrm{D}q/\mathrm{D}t = \Lambda d + v(\partial^2 \overline{U}/\partial y^2)$. The latter additional term is the advection of the mean flow vorticity by the cross-stream velocity perturbation. It is vital for the 2D optimal growth mechanism in the presence of an inflection point, e.g. Heifetz & Methven (2005); however, in figure 4(*c*) we can see that this term contributes almost nothing to the 3D growth mechanism.
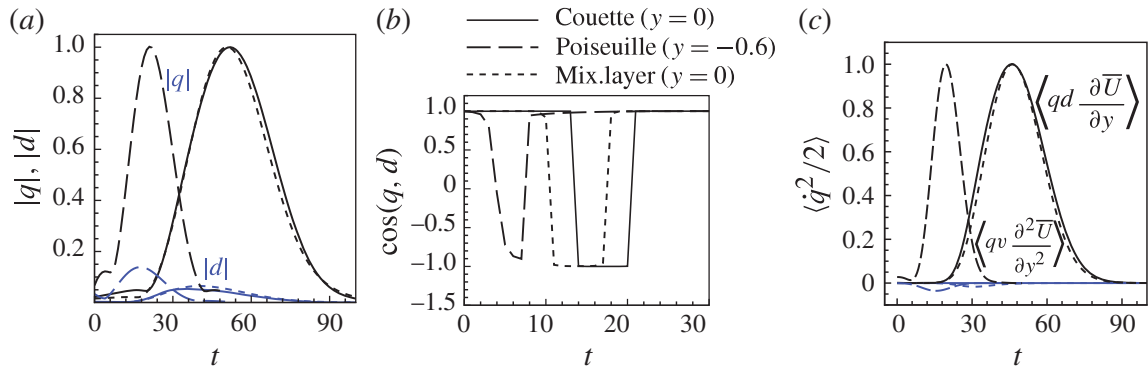
FIGURE 4. (Colour online) 3D growth of the planar divergent (d) and the spanwise vorticity (q) terms for the cases presented in figure 1, for Couette (solid), Poiseuille (long-dashed) and mixing-layer (short-dashed) profiles. (a) Evolution of the absolute values of the two fields. (b) The cosine of the phase shift between d and q at three selected levels (far enough from the boundaries) where the shear is positive and large. (c) Comparison between the two sources for growth of q, when the shear curvature is taken into account.

We now wish to focus on how the interplay between d and q affects the energy growth. Toward this end we invert d and q numerically to compute $\phi = \nabla_2^{-2}d$, and $\psi = \nabla_2^{-2}q$ in order to derive the divergent and vorticity-induced velocity fields according to (3.6). The contributions of the four terms of (3.10) to the energy growth are then computed and presented in figure 5.

A similar qualitative behaviour is identified for the three profiles. At the beginning, when the growth is mainly 2D, the Orr mechanism $-\langle u_q v_q \rangle$ dominates. Later on, when d amplifies q, the Orr mechanism increases accordingly but contributes toward a decay of the energy since the plane-wave-like structures are tilted with the shear. Hence for 3D growth, the Orr mechanism is mostly an energy sink rather than a source. At this stage the pure divergent contribution, $-\langle u_d v_d \rangle$, is positive as expected; however this contribution is relatively small since d itself remains small. It is clear from figure 5, and from the eddy geometry (figure 3), that the mixed term, $-\langle u_q v_d \rangle$, should be positive and large when the eddies are tilted strongly with the shear (the larger $-l$ becomes). This mixed term is responsible for most of the 3D optimal energy growth and is able to overwhelm the large negative contribution of the Orr mechanism. The last combined term, $-\langle u_d v_q \rangle$, is negative but relatively small since by then $k \ll |l|$. For comparison, for the 2D bounded Couette flow the amplitude of q remains constant (apart from small dissipation), and therefore energy growth and decay by the Orr mechanism should be almost symmetric. In figure 5 we also show the evolution of $-\langle u_q v_q \rangle$ for the 2D case presented in figure 1. It indeed maximizes when the eddies are tilted against the shear in an angle of $\pi/4$, vanishes when they become perpendicular to the shear and finally becomes negative, in an antisymmetric fashion, when tilted with the shear.

5. Conclusions and discussion

The energy growth mechanism which results from the Reynolds stress, $\langle -uv(\partial\overline{U}/\partial y)\rangle$, involves only the 2D shear plane dynamics, and is the same whether or not the perturbation itself is 2D or 3D. Nonetheless, the behaviour of the optimal energy growth in 2D is very different from that in 3D. This motivates us to re-examine the problem and seek an understanding which involves only the dynamics on the shear plane.
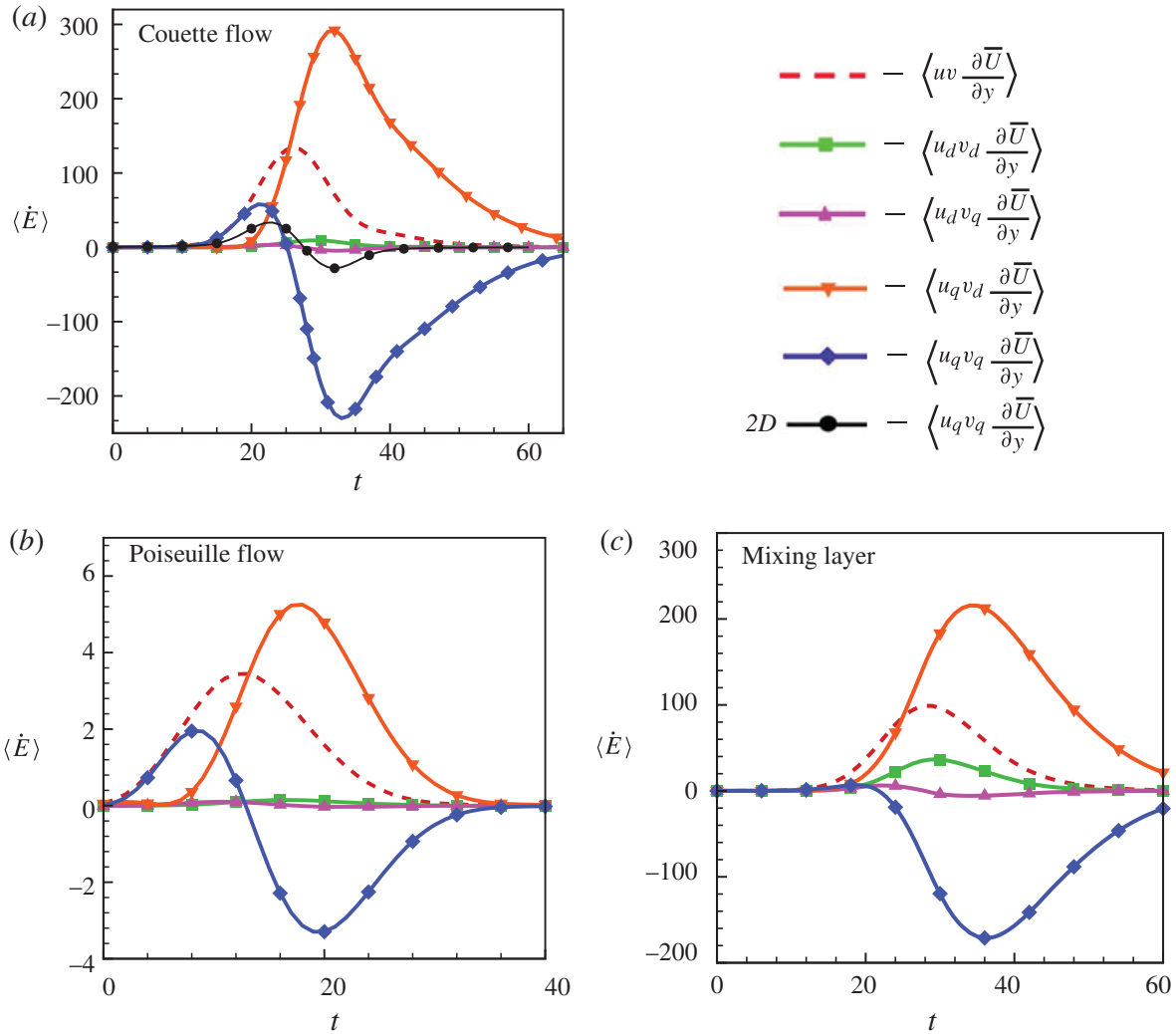
FIGURE 5. (Colour online) The various components of the Reynolds stress for the three 3D examples presented in figure 1: (*a*) Couette flow, (*b*) Poiseuiile flow, (*c*) mixing-layer flow. The behaviour is robust: at the beginning of the evolution, when the eddies are tilted against the shear, the growth is dominated by the Orr term, $-\langle u_q v_q \rangle$. When the eddies are turned to be tilted with the shear the Orr mechanism becomes the major energy sink (for the 2D dynamics in the Couette profile the Orr term is the only source for the Reynolds stress and it is presented for comparison in (*a*)). The pure divergent contribution, $-\langle u_d v_d \rangle$, turns from being negative to positive but remains small, while the mixed divergent rotational term, $-\langle u_d v_q \rangle$, changes sign from positive to negative but remains small as well. It is the other mixed term, $-\langle u_q v_d \rangle$, that becomes positive and large as the eddies become strongly tilted with the shear. Indeed the latter term is responsible for the large 3D optimal growth.

For incompressible flow the 2D dynamics results only from the rotational component (the spanwise vorticity) of the flow, whereas in 3D it results from both the rotational and the divergent components on the shear plane. A mutual growth of these two components explains why the 3D optimal growth is much larger than the 2D one. Numerical computations of the optimal dynamics for three different canonical profiles of plane parallel shear flows (Couette, Poiseuille, and mixing layer) reveal a generic behaviour of the perturbations at the stage of maximal growth. The perturbations are then organized as localized plane waves, in regions where the background shear is the largest. Furthermore, the waves are tilted with the shear, and the planar vorticity and divergence fields are in (out of) phase when the background shear is positive

(negative). This picture is very different from the optimal growth of 2D perturbations where energy grows when eddies are tilted against the shear.

While the divergent field affects the rotational one by vortex stretching in a straightforward manner, the growth mechanism of the planar divergent field is less obvious. It occurs when the pressure perturbation is negative and results both from a differential advection of background momentum by the perturbation field, and from a differential advection of perturbation momentum by the background flow. Indeed, a minimal model of a plane wave in an unbounded constant shear shows that mutual amplification of the divergent and rotational components may occur only when the waves are tilted with the shear. Such mutual growth is not enough by itself to ensure a large energy growth since the rotational Orr mechanism yields energy decay when the eddies are tilted with the shear. Decomposing the Reynolds stress in terms of the various contributions from the divergent and the rotational fields indicates that during the optimal evolution the mixed term $\langle -u_q v_d (\partial \overline{U}/\partial y) \rangle$ dominates the energy growth and overwhelms the decaying effect of the Orr mechanism.

The divergent–rotational interplay seems to occur in more complex setups. Pradeep & Hussain (2006) showed that there are two distinct mechanisms for transient growth in a vortex column: the 2D Orr mechanism and the growth of azimuthal stretching of spiral vortex filaments containing radial vorticity. From inspecting their simulations it seems that this mechanism is indeed the divergent–rotational one and it occurs when the filaments are tilted with the shear. In a following paper Hussain, Pradeep & Stout (2011) examined the nonlinear transient growth in a vortex column and found that the same 3D mechanism is responsible for the initial transient growth that generates new vortex threads, and hence leads to a cyclical energy growth that might sustain turbulence. Furthermore, Mao, Sherwin & Blackburn (2012) performed direct numerical simulations showing that the optimal 3D perturbation may cause a co-rotating vortex pair system to break up before a 2D merging occurs. It is interesting to examine whether the divergent–rotational interplay is responsible for this large 3D growth mechanism. Moreover, a 2D analogue of the 3D divergent–rotational interplay may occur in a 2D compressible flow. Chagelishvili *et al.* (1997), Farrell & Ioannou (2000) and Bakas (2009) showed that compressibility indeed leads to extraction of energy when the Orr waves are tilted with the shear.

The representation of the transient growth in terms of a mutual growth between the divergent and the rotational components can have direct implications for quasi-2D geophysical fluid dynamics where the rotational and the divergent (stretching) components are combined into a single variable – the potential vorticity (PV). Since transient growth occurs generically in such flows, and the nonlinear lifecycles of vortices, waves and jets are commonly analysed from the PV perspective, e.g. Methven *et al.* (2005), it will be interesting to decompose the non-modal PV dynamics and examine explicitly the interplay between the rotational and divergent components during the optimal evolution.

Since the Reynolds stress is the instantaneous source for energy growth in incompressible nonlinear flows, the linear analysis of optimal dynamics presented here may also have some relevance to nonlinear processes. We have shown that the vortex stretching mechanism which acts only in 3D, leads to the fundamentally different energy growth dynamics in 3D compared to 2D. Furthermore, vortex stretching also leads to the basic difference in the direction of energy cascade in 2D and 3D flows. One might argue then that in 2D, the Orr mechanism contributes to the inverse cascade since the maximum energy is attained when the cross-stream wavenumber vanishes, so that the total wavenumber decreases. In contrast, in 3D, the vortex stretching dynamics
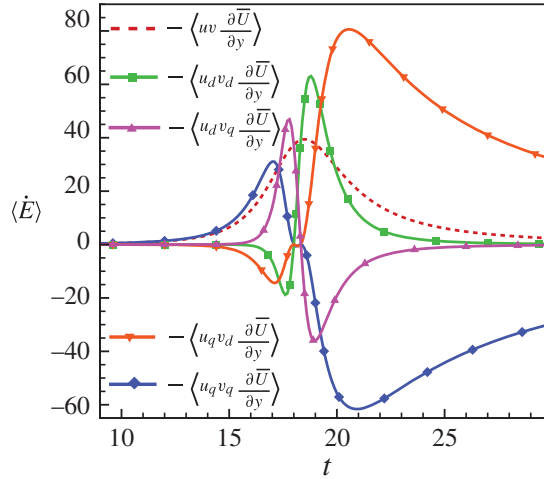
FIGURE 6. (Colour online) Same as in figure 5 but for the plane-wave solution of (A 1) and (A 2). The initial perturbation is normalized by the energy norm. The streamwise and spanwise wavenumbers $(k, m) = (0.5, 1)$, are as in the example for the Couette flow in figure 1. The initial cross-stream wavenumber is $l_0 = k \Lambda t_{perp} = 9$, where $\Lambda t_{perp} = 18$ is the normalized time by which the eddy streamwise vorticity contours become untilted in the bounded Couette simulation, presented in figure 1. At the stage of maximal growth figures 5 and 6 present a similar qualitative behaviour.

leads to amplification of energy when the cross-stream wavenumber is large, in line with the direct cascade mechanism.

Appendix. Analytical solution of a sheared plane wave in unbounded Couette flow

Define $\boldsymbol{K}_V^2 \equiv (k^2 + m^2)$, then the solution for (3.8) is:

$$\hat{q}(t) = \hat{q}_0 + \hat{d}_0 \Lambda t - \frac{m^2 \hat{p}_0}{2k^2 \Lambda} \frac{\boldsymbol{K}_0^4}{\boldsymbol{K}_V^2}$$

$$\times \left(\frac{\Lambda k l_0}{\boldsymbol{K}_0^2} t + \frac{l}{|\boldsymbol{K}_V|} \left[\arctan \left(\frac{l}{|\boldsymbol{K}_V|} \right) - \arctan \left(\frac{l_0}{|\boldsymbol{K}_V|} \right) \right] \right), \qquad \text{(A 1)}$$

$$\hat{d}(t) = \hat{d}_0 + \frac{m^2 \hat{p}_0}{2k \Lambda} \frac{\boldsymbol{K}_0^4}{\boldsymbol{K}_V^2}$$

$$\times \left(\frac{l}{\boldsymbol{K}^2} - \frac{l_0}{\boldsymbol{K}_0^2} + \frac{1}{|\boldsymbol{K}_V|} \left[\arctan \left(\frac{l}{|\boldsymbol{K}_V|} \right) - \arctan \left(\frac{l_0}{|\boldsymbol{K}_v|} \right) \right] \right), \qquad \text{(A 2)}$$

where $\hat{p} = (|\boldsymbol{K}_0|/|\boldsymbol{K}|)^4 \hat{p}_0$, and $\hat{v} = (|\boldsymbol{K}_0|/|\boldsymbol{K}|)^2 \hat{v}_0$.

As an example, the different components of the energy growth are presented in figure 6 for the plane-wave solution. The background shear and the streamwise and spanwise wavenumbers $(k, m) = (0.5, 1)$, are the same as in figure 1 for the 3D bounded Couette flow example. The initial cross-stream wavenumber $l_0 = k \Lambda t_{perp} = 9$, is chosen so that $l = 0$ corresponds to the normalized time $\Lambda t_{perp} = 18$, at which the optimal perturbation spanwise vorticity contours become perpendicular to the shear. Comparison between figures 5(a) and 6 reveals that, as expected, the plane wave does not mimic the energy growth when it is tilted against the shear. Nonetheless, at the stage of maximum growth the essence of the behaviour is similar, where

the mixed d–q term, $\langle -u_q v_d \Lambda \rangle$, overwhelms the negative contribution of the Orr mechanism $\langle -u_q v_q \Lambda \rangle$.

REFERENCES

BAKAS, N. A. 2009 Mechanisms underlying transient growth of planar perturbations in unbounded compressible shear flow. *J. Fluid Mech.* **639**, 479–507.

BUTLER, R. M. & FARRELL, B. F. 1992 Three-dimensional optimal perturbations in viscous shear flows. *Phys. Fluids* A **4**, 1367–1654.

CHAGELISHVILI, G. D., KHUJADZE, G. R., LOMINADZE, J. G. & ROGAVA, A. D. 1997 Acoustic waves in unbounded shear flows. *Phys. Fluids* **9**, 1955.

ELLINGSEN, T. & PALM, E. 1975 Stability of linear flow. *Phys. Fluids* **18**, 487.

FARRELL, B. F. & IOANNOU, P. J. 1993 Optimal excitation of three-dimensional perturbations in viscous constant shear flow. *Phys. Fluids* A **5**, 1390–1400.

FARRELL, B. F. & IOANNOU, P. J. 2000 Transient and asymptotic growth of two-dimensional perturbations in viscous compressible shear flow. *Phys. Fluids* **12**, 3021.

GELFGAT, A. YU. & KIT, E. 2006 Spatial versus temporal instabilities in a parametrically forced stratified mixing layer. *J. Fluid Mech.* **552**, 189–227.

HEIFETZ, E. & METHVEN, J. 2005 Relating optimal growth to counterpropagating Rossby waves in shear instability. *Phys. Fluids* **17**, 064107.

HUSSAIN, F., PRADEEP, D. S. & STOUT, E. 2011 Nonlinear transient growth in a vortex column. *J. Fluid Mech.* **682**, 304–331.

LANDAHL, M. T. 1980 A note on an algebraic instability of inviscid parallel shear flows. *J. Fluid Mech.* **98**, 243–251.

MAO, X., SHERWIN, S. J. & BLACKBURN, H. M. 2012 Non-normal dynamics of time-evolving co-rotating vortex pairs, *J. Fluid Mech.* (submitted).

METHVEN, J., HOSKINS, B. J., HEIFETZ, E. & BISHOP, C. H. 2005 The counter-propagating Rossby wave perspective on baroclinic instability. Part IV: nonlinear life cycles. *Q. J. R. Meteorol. Soc.* **131**, 1393–1424.

ORR, W. M. F. 1907 The stability or instability of the steady motions of a perfect liquid and of a viscous liquid. *Proc. R. Irish Acad.* A **27**, 69–138.

PRADEEP, D. S. & HUSSAIN, F. 2006 Transient growth of perturbations in a vortex column. *J. Fluid Mech.* **550**, 251–288.

REDDY, S. C. & HENNINGSON, D. S. 1993 Energy growth in viscous channel flows. *J. Fluid Mech.* **252**, 209–238.

SCHMID, P. J. & HENNINGSON, D. S. 2001 *Stability and Transition in Shear Flows*. Springer.